

A Novel Control Approach For Improved Performance of a High Power Factor Converter Under Supply and Load Perturbations

Deepak Sharma¹, Abdul Hamid Bhat², Aijaz Ahmad³

^{1,2,3}Department of Electrical Engineering, National Institute of Technology Srinagar, Kashmir

deepaksmail99@yahoo.com

Abstract— This paper presents a novel control approach for better performance of Three-phase Improved Power Quality Converters with supply and load perturbations. Space vector pulse width modulation algorithm has been used for the control of the Converter. The main goal of space vector PWM is to generate the PWM signals produced by time weights (t_a, t_b, t_0) of the nearest three vectors in the sector in which reference vector lies. The time intervals (t_a, t_b, t_0), determine the duration of the three nearest vectors that compose the switching sequence. The trajectory of reference vector is very important for SVPWM technique to obtain exact switching times of the nearest reference vectors under any perturbation. Due to supply or load perturbation, the trajectory of reference vector gets affected which results in deviating source side and load side parameters much beyond acceptable limits. In the proposed control approach, the space vector trajectory is made either large or small enough in each sector by the proposed algorithm so that the effects of a particular switching vector become prominent and power qualities at the source side and load side can be improved. The proposed control strategy takes into consideration the amount of deviation of Clarke Transformation parameters V_α, V_β and I_α, I_β during any perturbation. Accordingly parameters V_α, V_β are compensated as deviated from original values and line currents are modified in such a way that a required trajectory of the space vector can be generated. The proposed control algorithm retransforms the Clarke Transformation equations. The retransformation of Clarke Transformation generates a trajectory of required shape to vary time weight (t_a, t_b, t_0) of the three nearest vectors to overcome power quality issues for any perturbation. Three-Phase, IPQC system along with proposed control scheme is modeled in MATLAB/Simulink environment. Simulated results are presented to demonstrate the effectiveness of the proposed control technique and displays better performance with nearly unity input power factor, low input current THD and reduced ripple factor of the regulated DC output voltage under disturbed supply, which is regularly encountered in practical environment.

Index Terms— Power Quality, Improved Power Quality Converters, Multilevel Converters, Harmonics Compensation, Unbalanced AC Mains, Disturbed AC mains.

I. INTRODUCTION

Improved Power Quality AC/DC converters offer an attractive alternative for medium and higher power applications because of their various attractive features like better harmonic spectrum, lower di/dt and dv/dt stresses, lower EMI emissions and sometime suitability for operation at higher voltages. Space Vector Pulse Width Modulation (SVPWM) as shown in fig.1, has more recently been applied to converters because it offers the advantages of improved power quality and better DC-bus voltage utilization compared to sinusoidal PWM technique at same switching frequency. The most common types of power quality problems associated with IPQCs are like voltage sag, voltage swell, unbalanced supply, harmonics distortion, phase angle variations, frequency variations and load perturbation [27, 29]. Harmonic distortion and voltage sag power quality problems are more regularly encountered in practical environment. All these power qualities are defined by IEEE-1159(1995). Voltage sag is defined as a decrease in rms voltage to between 0.1 to 0.9 of nominal voltage at power frequency for duration of 0.5 cycle to 1 minute. Harmonic distortion is defined as voltage or current waveforms assuming non-sinusoidal shape. In presence of large number of nonlinear loads and their better controlled use, non-conventional power production technologies such as

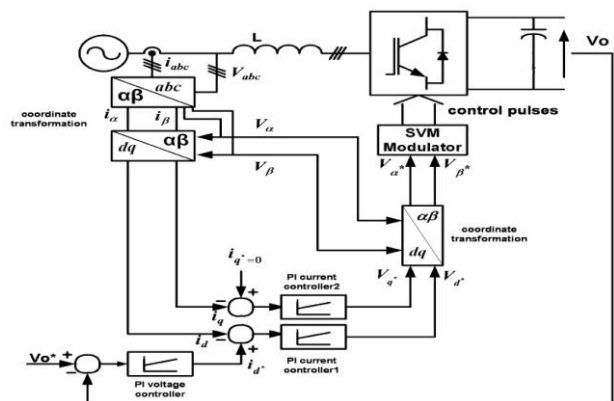


Fig.1 Block diagram of voltage-oriented control scheme.

solar and wind power and the various power electronics devices used in the system introduce harmonic voltage/current distortion. Harmonics waveforms correspond to the sum of different sine-waves with different magnitude and phase, having frequencies that are multiples of power-system frequency. Voltage unbalance is defined as voltage variation in a three-phase system in which the three voltage magnitudes are not equal [3,4]. In the literature, limited work has been reported to mitigate the effects of load and supply perturbations on converters. Most related work is based on detection and classification of the unbalanced supply in power system [10-26]. There are some schemes reported in the literature to overcome the problem of unbalanced supply by providing insensitivity towards supply disturbances within certain limited ranges [27-35]. From the literature some work for the protection of sensitive loads Dynamic voltage restorer is used from harmonic distortion, sag/swell, and unbalance in supply voltage economically [30-32]. In [33] authors proposed a novel algorithm based on the dot product of three dimensional space vectors in the abc coordinate system, for real time calculation of the instantaneous positive, negative and zero sequence components for each individual harmonic for compensating fundamental reactive power, selected current harmonics and current unbalances. This method is computationally simple and requires no coordinate transformation. In [34] authors have used concept of multilevel converts for reactive power compensation. In [35] the scheme is based on maintaining circular trajectory of the space vector even under disturbed supply using inverse Clarke Transformation. But no compensation technique is reported for optimising the performance of the converter using SVPWM under power quality problems.

These non-ideal conditions are regularly encountered in practical operating conditions resulting in the deteriorating performance of converter in real time applications. The stable operation of the IPQC under disturbed mains condition is a burning issue and has been a topic of intensive international research. In this paper, an attempt has been made to minimize the effect of source and load perturbations on IPQCs so has to maintain source and load parameters within acceptable limits i.e. nearly unity input power factor, low input current THD and reduced ripple factor of the regulated DC output voltage.

II. MATHEMATICAL MODELING UNDER SUPPLY PERTURBATIONS

Space Vector Pulse Width Modulation scheme for three-phase IPQC is shown in fig 1. Under balanced three phase sinusoidal voltages, V_s is a rotating vector called reference vector, which forms a circular trajectory in shape in the complex ($\alpha - \beta$) plane at a constant amplitude with fundamental angular speed. This circular trajectory is sampled instantly in each 60° in order to have 6 active vectors for two level three-phase rectifiers as shown in Fig.2.

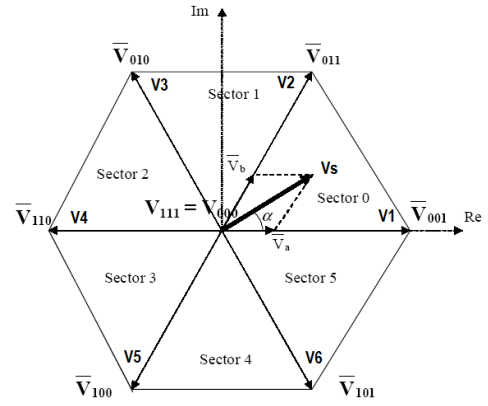


Fig 2: Rotating reference vector

There are six active vectors and two non-active vectors or null states (000,111). So there are eight basic space vectors. There are only eight possible switching states depending on the six devices that are turned ON as shown in table 1. This table expresses the allowed switching states in each sector of the space vector. This continuously rotating vector V_s inside the hexagon must complete one complete turn with angular velocity which depends upon the supply frequency.

State	Device Conducting
000	T2,T4,T6
001	T2,T4,T5
010	T2,T3,T6
011	T2,T3,T5
100	T1,T4,T6
101	T1,T4,T5
110	T1,T3,T6
111	T1,T3,T5

Table1. Three-phase converter switching states.

Space Vector PWM generates PWM signals for the converter by appropriate time weightage of the two reference vectors that in a sector in which space vector (V_s) lies. Assuming the reference vector to be located in "sector 0" as shown in the Fig.2, the reference vector V_s can be expressed by appropriate time weightage of the two reference vectors as,

$$V_s = \bar{V}_a + \bar{V}_b \quad (1)$$

where \bar{V}_a and \bar{V}_b are respectively components of vector V_s with respect to V_1 (i.e. \bar{V}_{001}) and V_2 (i.e. \bar{V}_{011}). For a modulation period or PWM period (T_0), \bar{V}_a and \bar{V}_b are generated by applying well defined percentage of T_0 for reference vectors V_1 (i.e. \bar{V}_{001}) and V_2 (i.e. \bar{V}_{011}).

$$V_s = \bar{V}_a + \bar{V}_b = \frac{ta}{T_0} (V_1 \text{ or } \bar{V}_{001}) + \frac{tb}{T_0} (V_2 \text{ or } \bar{V}_{011}) +$$

$$\frac{t0}{T_0} (V_0/V_7 \text{ or } \bar{V}_{000} / \bar{V}_{111}) \quad (2)$$

$$ta = \frac{V_a}{V_1} T_0, \quad tb = \frac{V_b}{V_2} T_0 \text{ and } t0 = T_0 - ta - tb \quad (3)$$

Applying the trigonometric relation in Fig.2 we have,

$$V_s \sin\left(\frac{\pi}{3} - \alpha\right) = V_a \sin\left(\frac{\pi}{3}\right)$$

$$\text{and } V_s \sin\alpha = V_b \sin\left(\frac{\pi}{3}\right) \quad (4)$$

Therefore we can have

$$V_a = \frac{2}{\sqrt{3}} V_s \sin\left(\frac{\pi}{3} - \alpha\right) \quad \text{and} \quad V_b = \frac{2}{\sqrt{3}} V_s \sin\alpha \quad (5)$$

Substituting the values of V_a, V_b in equation (3) it is possible to calculate t_a, t_b and t_o for any sector (i.e. with respect to vector reference angle ' α ') and modulation index (modulation index ' m ' = V_s/V_{dc}) where V_{dc} is constant value.

For vector positions between $0 \leq \alpha \leq \frac{\pi}{3}$

$$t_a = \frac{2}{\sqrt{3}} T_0 \cdot m \cdot \sin\left(\frac{\pi}{3} - \alpha\right), \quad t_b = \frac{2}{\sqrt{3}} T_0 \cdot m \cdot \sin\alpha \quad \text{and} \\ t_o = T_0 - t_a - t_b \quad (6)$$

If ' m ' is varied in each sector of space vector, then t_a, t_b, t_o also change for that sector. This will result in the varying the conducting times of the devices under the influence of the space vector. If control on the device conducting time can be made, power quality can be achieved under supply disturbance conditions. Since Modulation index $m = V_s/V_{dc}$ and V_{dc} is constant, the only way left is to vary the ' V_s ' magnitude as required in each sector. In other words, if the trajectory of the V_s changes, then t_a, t_b, t_o will also change. The proposed algorithm is used here to obtain exact switching times of the devices for any supply conditions but keeping the sampling times same for each sector. The exact needed switching of the devices will be responsible to maintain parameters within acceptable limits for source side in terms of unity power factor, low input current THD and for load side are in terms of reduced-rippled, well-regulated DC-bus voltage. Reference vector trajectory shape in each sector will predict exact switching under any supply conditions. According to supply conditions, the proposed controller will form a required reference space vector trajectory for a particular sector of SVPWM.

II a) Effect of Disturbed Supply (i.e. unbalanced supply and injected harmonics) on IPQC

The effect of disturbed supply can be severe on equipment such as induction motors, power electronic converters and adjustable speed drives (ASDs). Power electronic converters serve as the interface for many large electronic loads ranging from three-phase uninterruptible power supplies to motors operating at variable speeds through the use of adjustable speed drives. Most of these converters contain a diode front-end rectifier and DC-link capacitor to convert the incoming AC voltage to a low-ripple DC voltage.

As the input voltage unbalance increases, the input current becomes significantly more unbalanced due to the asymmetric conduction of the diodes. The voltage unbalance may cause excessive current in one or two phases, which can trip overload-protection circuits. The increased current can also cause excess heating of the diodes and decrease the life of the capacitor or require the use of a larger capacitor. Under unbalanced supply condition, it has been observed that even and odd harmonics are generated and their magnitudes are in

proportion to the difference in AC supply. Bi-directional Three-phase boost converter topology is shown in fig.3.

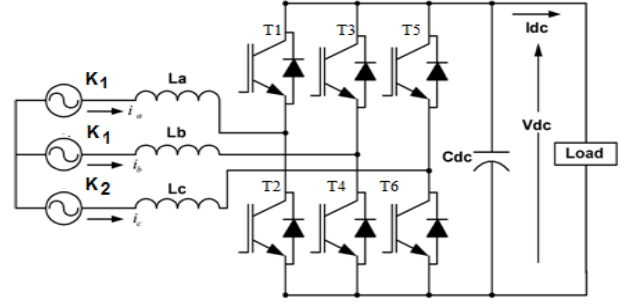


Fig. 3 Bi-directional Three-phase boost converter topology

Three-phase input supply can be written as

$$x_1(t) = K_1 \sin(\omega t + 120^\circ) \\ x_2(t) = K_1 \sin(\omega t - 120^\circ) \quad (7) \\ x_3(t) = K_2 \sin(\omega t)$$

where k_1, k_2 are the magnitude terms and $k_2 < k_1$

Considering IPQC as a symmetrical third-order transfer function,

$$h(t) = a_0 + a_1 x_1(t) + a_2 x_2(t) + a_3 x_3(t) \quad (8)$$

where, a_0, a_1, a_2 , represent a third-order system, then

$$y(t) = h(x_1(t)) - h(x_2(t)) - h(x_3(t)) \quad (9)$$

where, $y(t)$ is the differential output signal.

$$y(t) = a_1[x_1(t) - x_2(t) - x_3(t)] + a_2[x_1^2(t) - x_2^2(t) - x_3^2(t)] + a_3[x_1^3(t) - x_2^3(t) - x_3^3(t)] \quad (10)$$

Applying trigonometric formula yields,

$$a_1[x_1(t) - x_2(t) - x_3(t)] = a_1[2k_1 \cos \omega t \sin 120^\circ - k_2 \sin \omega t] \quad (11)$$

$$a_2[x_1^2(t) - x_2^2(t) - x_3^2(t)] = a_2[k_1^2 \sin 2\omega t \sin 240^\circ - \frac{k_2^2}{2} [1 - \cos 2\omega t]] \quad (12)$$

$$a_3[x_1^3(t) - x_2^3(t) - x_3^3(t)] = a_3[\frac{3}{2} k_1^3 \cos \omega t \sin 120^\circ - \frac{k_1^3}{2} \cos 3\omega t \sin 360^\circ - k_2^3 \frac{3}{4} \sin \omega t + \frac{k_2^3}{4} \sin 3\omega t] \quad (13)$$

Now substituting the equations 11, 12, 13 in equation 10, we get

$$y(t) = a_1[2k_1 \cos \omega t \sin 120^\circ - k_2 \sin \omega t] + a_2[k_1^2 \sin 2\omega t \sin 240^\circ - \frac{k_2^2}{2} [1 - \cos 2\omega t]] + a_3[\frac{3}{2} k_1^3 \cos \omega t \sin 120^\circ - \frac{k_1^3}{2} \cos 3\omega t \sin 360^\circ - k_2^3 \frac{3}{4} \sin \omega t + \frac{k_2^3}{4} \sin 3\omega t] \quad (14)$$

From equation (14), we conclude that even and odd harmonics are proportional to the difference in the magnitudes of phase voltage (k_1 and k_2) and vice versa.

II b) Effect of Phase Imbalance on IPQC

Three-phase input supply having phase imbalance can be written as

$$\begin{aligned}
x_1(t) &= K \sin(\omega t + \phi_1) \\
x_2(t) &= K \sin(\omega t - \phi_2) \\
x_3(t) &= K \sin(\omega t)
\end{aligned} \tag{15}$$

where k are the phase voltage magnitude terms and ϕ_1, ϕ_2 can have any value range from +120 to -120
Considering IPQC as a symmetrical third-order transfer function

$$h(t) = a_0 + a_1 x_1(t) + a_2 x_2(t) + a_3 x_3(t) \tag{16}$$

where, $a_0, a_1, a_2,$ represents a third-order system, then

$$\begin{aligned}
y(t) &= a_1 [x_1(t) - x_2(t) - x_3(t)] + a_2 [x_1^2(t) - x_2^2(t) - x_3^2(t)] + a_3 [x_1^3(t) - x_2^3(t) - x_3^3(t)] \\
&= a_1 [K \sin(\omega t + \phi_1) - K \sin(\omega t - \phi_2) - K \sin(\omega t)] \\
&= Ka_1 [\sin(\cos\phi_1 - \phi_2) + \cos\omega t(\sin\phi_1 + \sin\phi_2) - \sin(\omega t)] \\
&= a_2 [x_1^2(t) - x_2^2(t) - x_3^2(t)] \\
&= a_2 [K^2 \sin^2(\omega t + \phi_1) - K^2 \sin^2(\omega t - \phi_2) - K^2 \sin^2(\omega t)] \\
&= a_2 K^2 [\sin^2(\omega t + \phi_1) - \sin^2(\omega t - \phi_2) - \sin^2(\omega t)]
\end{aligned} \tag{17}$$

$$\begin{aligned}
&a_1 [x_1(t) - x_2(t) - x_3(t)] = \\
&a_1 [K \sin(\omega t + \phi_1) - K \sin(\omega t - \phi_2) - K \sin(\omega t)] \\
&= Ka_1 [\sin(\cos\phi_1 - \phi_2) + \cos\omega t(\sin\phi_1 + \sin\phi_2) - \sin(\omega t)] \\
&= a_2 [x_1^2(t) - x_2^2(t) - x_3^2(t)] \\
&= a_2 [K^2 \sin^2(\omega t + \phi_1) - K^2 \sin^2(\omega t - \phi_2) - K^2 \sin^2(\omega t)] \\
&= a_2 K^2 [\sin^2(\omega t + \phi_1) - \sin^2(\omega t - \phi_2) - \sin^2(\omega t)]
\end{aligned} \tag{18}$$

$$a_2 [x_1^2(t) - x_2^2(t) - x_3^2(t)] \tag{20}$$

$$\begin{aligned}
&= a_2 [K^2 \sin^2(\omega t + \phi_1) - K^2 \sin^2(\omega t - \phi_2) - K^2 \sin^2(\omega t)] \\
&= a_2 K^2 [\sin^2(\omega t + \phi_1) - \sin^2(\omega t - \phi_2) - \sin^2(\omega t)]
\end{aligned} \tag{21}$$

$$\text{but } \sin^2 \omega t = \frac{1}{2} - \frac{\cos 2\omega t}{2} \tag{22}$$

$$\begin{aligned}
&= a_2 K^2 \left[\left\{ \frac{1}{2} - \frac{\cos 2(\omega t + \phi_1)}{2} \right\} - \left\{ \frac{1}{2} - \frac{\cos 2(\omega t - \phi_2)}{2} \right\} - \left\{ \frac{1}{2} - \frac{\cos 2\omega t}{2} \right\} \right] \\
&= a_2 K^2 \left[-\frac{1}{2} \cos 2(\omega t + \phi_1) + \frac{1}{2} \cos 2(\omega t - \phi_2) - \frac{1}{2} + \frac{1}{2} \cos 2\omega t \right]
\end{aligned} \tag{23}$$

$$\begin{aligned}
&= a_2 K^2 \left[-\frac{1}{2} \cos 2(\omega t + \phi_1) + \frac{1}{2} \cos 2(\omega t - \phi_2) - \frac{1}{2} + \frac{1}{2} \cos 2\omega t \right] \\
&= a_3 [x_1^3(t) - x_2^3(t) - x_3^3(t)] \\
&= a_3 [K^3 \sin^3(\omega t + \phi_1) - K^3 \sin^3(\omega t - \phi_2) - K^3 \sin^3(\omega t)] \\
&= a_3 [K^3 \left\{ \frac{3}{4} \sin(\omega t + \phi_1) - \frac{1}{4} \sin 3(\omega t + \phi_1) \right\} - K^3 \left\{ \frac{3}{4} \sin(\omega t - \phi_2) - \frac{1}{4} \sin 3(\omega t - \phi_2) \right\} - K^3 \left\{ \frac{3}{4} \sin \omega t - \frac{1}{4} \sin 3\omega t \right\}]
\end{aligned} \tag{24}$$

$$a_3 [x_1^3(t) - x_2^3(t) - x_3^3(t)] \tag{25}$$

$$\begin{aligned}
&= a_3 [K^3 \sin^3(\omega t + \phi_1) - K^3 \sin^3(\omega t - \phi_2) - K^3 \sin^3(\omega t)] \\
&= a_3 [K^3 \left\{ \frac{3}{4} \sin(\omega t + \phi_1) - \frac{1}{4} \sin 3(\omega t + \phi_1) \right\} - K^3 \left\{ \frac{3}{4} \sin(\omega t - \phi_2) - \frac{1}{4} \sin 3(\omega t - \phi_2) \right\} - K^3 \left\{ \frac{3}{4} \sin \omega t - \frac{1}{4} \sin 3\omega t \right\}]
\end{aligned} \tag{26}$$

$$\text{but } \sin^3 x = \frac{3}{4} \sin x - \frac{1}{4} \sin 3x \tag{27}$$

$$\begin{aligned}
&= a_3 [K^3 \left\{ \frac{3}{4} \sin(\omega t + \phi_1) - \frac{1}{4} \sin 3(\omega t + \phi_1) \right\} - K^3 \left\{ \frac{3}{4} \sin(\omega t - \phi_2) - \frac{1}{4} \sin 3(\omega t - \phi_2) \right\} - K^3 \left\{ \frac{3}{4} \sin \omega t - \frac{1}{4} \sin 3\omega t \right\}] \\
&= a_3 \left[\frac{3}{4} K^3 \sin(\omega t + \phi_1) - \frac{1}{4} K^3 \sin 3(\omega t + \phi_1) - \frac{3}{4} K^3 \sin(\omega t - \phi_2) + \frac{1}{4} K^3 \sin 3(\omega t - \phi_2) - \frac{3}{4} K^3 \sin \omega t + \frac{1}{4} K^3 \sin 3\omega t \right]
\end{aligned} \tag{28}$$

$$\begin{aligned}
&= a_3 \left[\frac{3}{4} k^3 \sin \omega t \cos \phi_1 + \frac{3}{4} k^3 \cos \omega t \sin \phi_1 - \frac{k^3}{4} \sin 3\omega t \cos 3\phi_1 - \frac{k^3}{4} \cos 3\omega t \sin 3\phi_1 - \frac{3}{4} k^3 \sin \omega t \cos \phi_2 + \frac{k^3}{4} \sin 3\omega t \cos \phi_2 - \frac{k^3}{4} \cos 3\omega t \sin 3\phi_2 - \frac{3}{4} k^3 \sin \omega t + \frac{k^3}{4} \sin 3\omega t \right] \\
&= a_3 \left[\frac{3}{4} k^3 \left[3 \sin \omega t \cos \phi_1 + 3 \cos \omega t \sin \phi_1 - \sin 3\omega t \cos 3\phi_1 - \cos 3\omega t \sin 3\phi_1 - 3 \sin \omega t \cos \phi_2 + 3 \cos \omega t \sin \phi_2 + \sin 3\omega t \cos 3\phi_2 - \cos 3\omega t \sin 3\phi_2 - 3 \sin \omega t + \sin 3\omega t \right] \right]
\end{aligned} \tag{29}$$

Substituting (19),(24) and (30) in equation(17) we have

$$\begin{aligned}
y(t) &= Ka_1 [\sin(\cos\phi_1 - \phi_2) + \cos\omega t(\sin\phi_1 + \sin\phi_2) - \sin(\omega t)] + a_2 K^2 \left[-\frac{1}{2} \cos 2(\omega t + \phi_1) + \frac{1}{2} \cos 2(\omega t - \phi_2) - \frac{1}{2} + \frac{1}{2} \cos 2\omega t \right] \\
&+ k^3 [3 \sin \omega t \cos \phi_1 + 3 \cos \omega t \sin \phi_1 - \sin 3\omega t \cos 3\phi_1 - \cos 3\omega t \sin 3\phi_1 - 3 \sin \omega t \cos \phi_2 + 3 \cos \omega t \sin \phi_2 + \sin 3\omega t \cos 3\phi_2 - \cos 3\omega t \sin 3\phi_2 - 3 \sin \omega t + \sin 3\omega t] \\
&= a_2 K^2 \left[-\frac{1}{2} \cos 2(\omega t + \phi_1) + \frac{1}{2} \cos 2(\omega t - \phi_2) - \frac{1}{2} + \frac{1}{2} \cos 2\omega t \right] + k^3 [3 \sin \omega t \cos \phi_1 + 3 \cos \omega t \sin \phi_1 - \sin 3\omega t \cos 3\phi_1 - \cos 3\omega t \sin 3\phi_1 - 3 \sin \omega t \cos \phi_2 + 3 \cos \omega t \sin \phi_2 + \sin 3\omega t \cos 3\phi_2 - \cos 3\omega t \sin 3\phi_2 - 3 \sin \omega t + \sin 3\omega t] \\
&= a_2 K^2 \left[-\frac{1}{2} \cos 2(\omega t + \phi_1) + \frac{1}{2} \cos 2(\omega t - \phi_2) - \frac{1}{2} + \frac{1}{2} \cos 2\omega t \right] + k^3 [3 \sin \omega t \cos \phi_1 + 3 \cos \omega t \sin \phi_1 - \sin 3\omega t \cos 3\phi_1 - \cos 3\omega t \sin 3\phi_1 - 3 \sin \omega t \cos \phi_2 + 3 \cos \omega t \sin \phi_2 + \sin 3\omega t \cos 3\phi_2 - \cos 3\omega t \sin 3\phi_2 - 3 \sin \omega t + \sin 3\omega t]
\end{aligned} \tag{30}$$

From Equation (33), the n^{th} order of harmonic amplitude is proportional to the n^{th} magnitude of $k(\text{phase voltage})$,

$$\text{i.e. } n^{\text{th}} \text{ harmonic} \propto k^n \tag{32}$$

Equation (31) shows that the n^{th} -harmonic is severely affected by phase imbalance. From equations (14) and (31), we conclude that that the n^{th} order of harmonic is more severely affected by phase imbalance than by magnitude imbalance. For phase imbalance, even and odd harmonic are proportional to the n^{th} multiplication of phase voltage (k), while for magnitude imbalance, the n^{th} order of the harmonic is proportional to the difference of the squares of k_1 and $k_2(\text{phase voltage difference})$.

III. PROPOSED CONTROL ALGORITHM

To overcome power quality issue for supply and load perturbation, new technique is proposed to generate exact switching time weights (t_a, t_b, t_0), which determine the duration of the three vectors that compose the switching sequence for any supply conditions but keeping the sampling times same for each sector. The proposed algorithm retransforms the Clarke Transformation. The detailed working of the proposed algorithm is as shown in fig.4. The proposed algorithm is based on retransformation of Clarke Transformation. Retransformed Clarke Transformation is used to form a required reference space vector trajectory for any perturbations to maintain power quality at the source side and as well as load side. The required trajectory shape of the reference vector is needed to change the duty ratio by varying the time weights (t_a, t_b, t_0) of the nearest three vectors in the sector in which reference vector lies. This action will overcome power quality issues under supply and load perturbation.

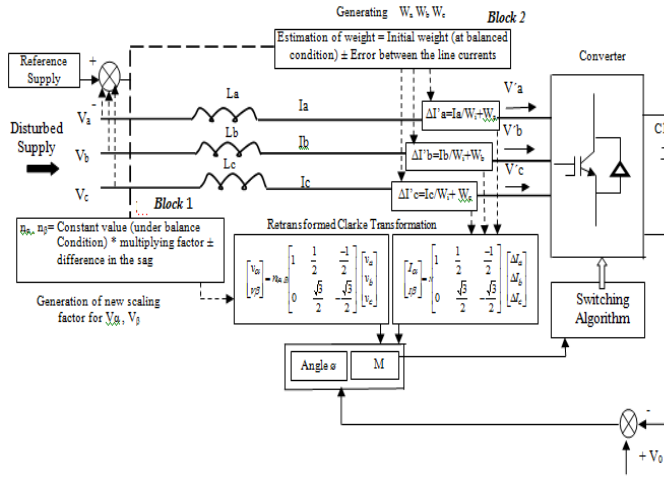


Fig: 4 proposed Control Algorithm

Formation of required trajectory of reference vector

The change in the supply conditions affects the magnitude of V_α, V_β and I_α, I_β of Clarke Transformation which further affects the rotating frame of reference (d-q) components, which are responsible for the formation of reference rotating space vector. Fig.4b depicts the change in the magnitude of the V_α and V_β under disturbed supply condition.

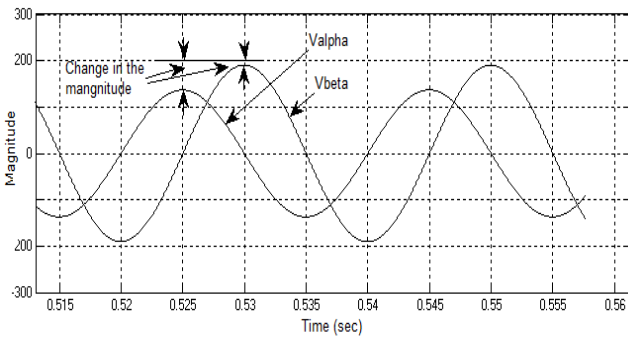


Fig. 4b Change in the magnitude of the V_α and V_β

Due to change in V_α, V_β and I_α, I_β of Clarke Transformation, reference vector trajectory changes from circular to irregular circular. In other words, if the magnitude of the reference is different in each sector, it will affect the duty ratios of nearest three vectors due to change in t_a, t_b, t_c . At the same time, it keeps the total sum of the duty ratios in the each sector same (i.e. $t_a + t_b + t_c = \text{constant value}$). Therefore, duty ratio in each sector will either be increased or decreased unsymmetrically which results in deterioration of quality of source currents and a large stress on power semiconductor devices. But under disturbed supply conditions, if the switching ratio of switching state is changed in some symmetrical ways depending upon the required duty ratio of t_a, t_b, t_c , then improved power quality at the source side and load side can be achieved.

III a). Computation of the compensation in voltage vector of Clarke Transformation

The function of the block 1 is to nullify the effect on voltage vector of Clarke Transformation caused by disturbed supply conditions (unbalanced voltage or injected harmonics). Under disturbed supply conditions,

$$V' = V'a + V'b\alpha + V'c\alpha^2 \quad (35)$$

where $V'a, V'b, V'c$ are the actual disturbed supply fed to the converter.

$$V' = V'\alpha + jV'\beta \quad (36)$$

$$\text{where } V'\alpha = \frac{2}{3} \left(V'a - \frac{1}{2}V'b - \frac{1}{2}V'c \right) \quad (37)$$

$$\text{and } V'\beta = \frac{2}{3} \left(\frac{\sqrt{3}}{2}V'b - \frac{3}{2}V'c \right) \quad (38)$$

now, $V - V' = L \frac{\Delta I}{\Delta T}$, where $V - V' = \text{Disturbed supply}$ (39)

From equation (39), adding or subtracting the compensating value of V_α and V_β with scaling factors in proportion to change in the magnitudes of the V_α, V_β results in nullifying the effect on V_α, V_β of the Clarke Transformation as given in equation in (40), such that V' is made equal to V . This compensation value is generated in the block 1 of the proposed control technique.

$$\begin{bmatrix} v_\alpha \\ v_\beta \end{bmatrix} = \frac{2}{3} \begin{bmatrix} 1 & \frac{1}{2} & -\frac{1}{2} \\ 0 & \frac{\sqrt{3}}{2} & -\frac{\sqrt{3}}{2} \end{bmatrix} \begin{bmatrix} v_a \\ v_b \\ v_c \end{bmatrix} \quad (40)$$

The compensating values for n_α, n_β can be calculated in proportion to any change in the supply. These proportional values are formulated by,

Compensated value can be formulated as $n_{(\alpha, \beta)} = \text{Constant value (under balance condition)} \times \text{multiplying factor} \pm \text{difference in input signal}$. (41)

With the evolution of new values for $n_{(\alpha, \beta)}$ voltage vector of Clark Transformation will Retransform the Clark Transformation (28) to absorb any change in V_α, V_β .

$$\begin{bmatrix} v_\alpha \\ v_\beta \end{bmatrix} = n_{(\alpha, \beta)} \begin{bmatrix} 1 & \frac{1}{2} & -\frac{1}{2} \\ 0 & \frac{\sqrt{3}}{2} & -\frac{\sqrt{3}}{2} \end{bmatrix} \begin{bmatrix} v_a \\ v_b \\ v_c \end{bmatrix} \quad (42)$$

$$\text{now we have, } V = L \frac{\Delta I}{\Delta T} \quad (43)$$

The next step is to form a required trajectory of the reference vector from retransformation of current vector of Clark Transformation. The detailed working is defined in block 2.

IIIb). Generating of required trajectory of reference vector

The function of this block2 is to generate a trajectory according to the required duty ratio for T_a, T_b, T_c .

$$\Delta I = I' - I = \text{Change in the line currents.}$$

$$\Delta I (\text{Current error vector}) = (\Delta I_a, \Delta I_b, \Delta I_c) \quad (44)$$

$$\Delta T = \Delta T_0 + \Delta T_1 + \Delta T_2. \quad (45)$$

where, ΔT is same duty ratio, but formed by new magnitudes of T_0, T_1 and T_2

Equation (45) represents current error vector formed due to difference in each line current magnitude. This difference is due to non uniform conduction of the devices (i.e. irregular shape of the trajectory). If each line current error ($\Delta I_a, \Delta I_b, \Delta I_c$) is computed separately so that a required regulated trajectory can be formulated to compensate generated reactive power, minimized current error vector is resulted and better power quality can be achieved at the source side and load side. The error computed will form a required space vector trajectory, so as to have new duty cycle in each sector with same sampling time. The change of duty cycle will help to attain lag angle between the supply voltage vector and reference current vector to compensate reactive power

generated under disturbed supply conditions. Each line current error is computed in the block (2) of the proposed control technique.

Now, $\Delta I =$ Current error vector ($\Delta I_a, \Delta I_b, \Delta I_c$) is formed due to difference in line currents. Each line currents error ($\Delta I'_a, \Delta I'_b, \Delta I'_c$) is computed by the following equations

$$\begin{aligned}\Delta I'_a &= \Delta I_a / W_a + W_i \\ \Delta I'_b &= \Delta I_b / W_b + W_i \\ \Delta I'_c &= \Delta I_c / W_c + W_i\end{aligned}\quad (46)$$

where, W_i empirical initial weight adjusted during balanced supply conditions and W_a, W_b, W_c are proportional values formulated as,

Estimation of weight (W_a, W_b, W_c) = Initial weight (at balanced condition) \pm Error between the line currents (47)

The conventional Clarke Transformation as given in equation in (48). It is retransformed after computing each line current

$$\begin{bmatrix} I_\alpha \\ I_\beta \end{bmatrix} = n_{(\alpha, \beta)} \begin{bmatrix} 1 & \frac{1}{2} & \frac{-1}{2} \\ 0 & \frac{\sqrt{3}}{2} & \frac{-\sqrt{3}}{2} \end{bmatrix} \begin{bmatrix} I_a \\ I_b \\ I_c \end{bmatrix}\quad (48)$$

error ($\Delta I_a, \Delta I_b, \Delta I_c$) as given in the equation (49) to generate a trajectory according to the required duty ratio for T_a, T_b, T_c .

$$\begin{bmatrix} I_\alpha \\ I_\beta \end{bmatrix} = N \begin{bmatrix} 1 & \frac{1}{2} & \frac{-1}{2} \\ 0 & \frac{\sqrt{3}}{2} & \frac{-\sqrt{3}}{2} \end{bmatrix} \begin{bmatrix} \Delta I_a \\ \Delta I_b \\ \Delta I_c \end{bmatrix}\quad (49)$$

After applying both steps of the proposed algorithm, the magnitude of the reference vector is given by,

$$V_s \left(\frac{\Delta T}{\Delta I} \right) = V_a \left(\frac{T_a}{\Delta T} \frac{I_a}{\Delta I_a} \right) + V_b \left(\frac{T_b}{\Delta T} \frac{I_b}{\Delta I_b} \right) + V_c \left(\frac{T_c}{\Delta T} \frac{I_c}{\Delta I_c} \right)\quad (50)$$

$$\text{Since, } V_s = M V_{dc}\quad (51)$$

$$M = V_s / V_{dc}\quad (52)$$

where M is the modulation index and V_{dc} is the desired constant dc voltage.

Since modulation index is varied in each region, $\Delta T_a, \Delta T_b$ and ΔT_c will be different from the previous region resulting in the stable working of the converter.

IV. PERFORMANCE EVALUATION

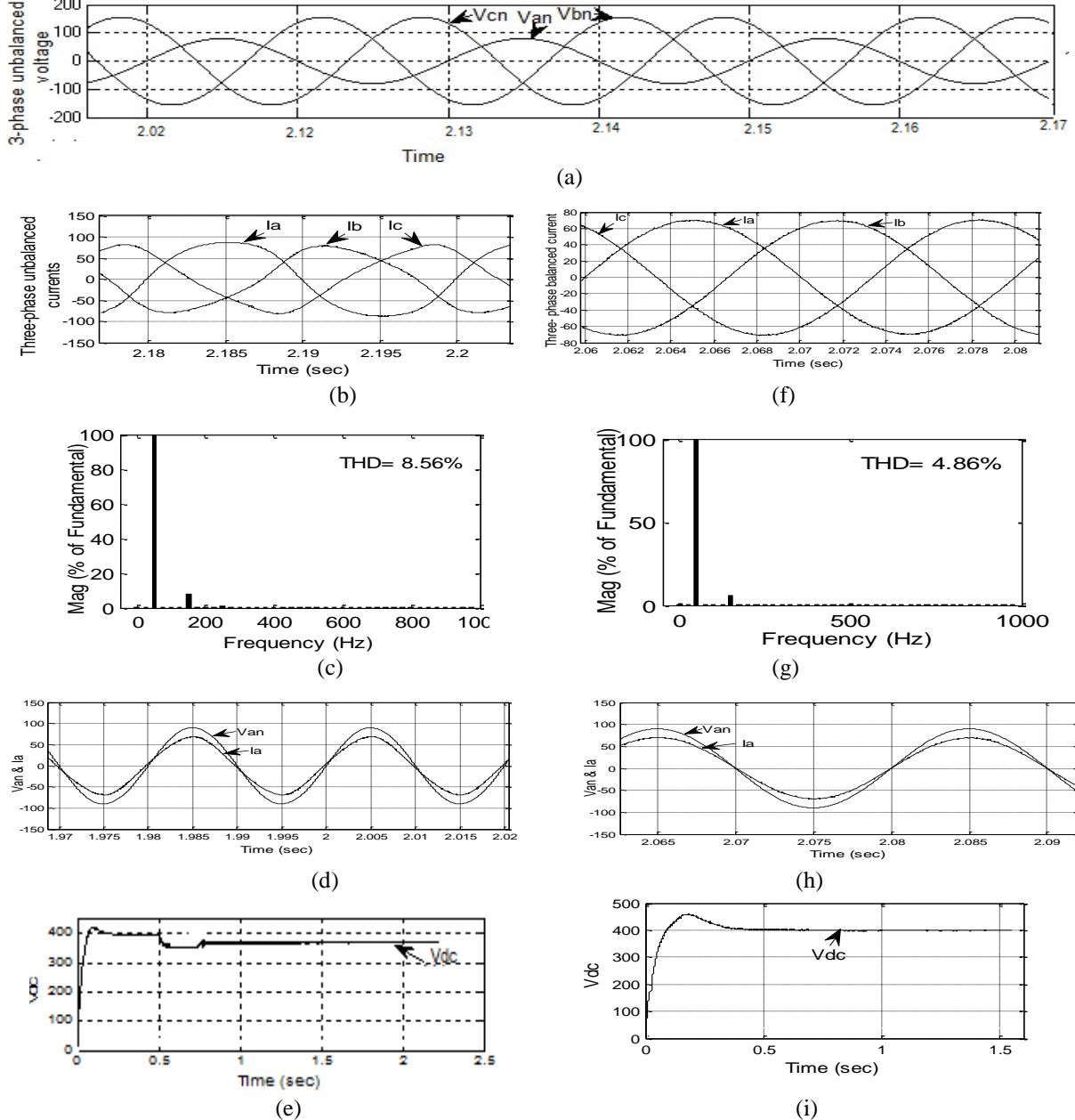
The performance of traditionally controlled IPQC and IPQC with the proposed control algorithm under unbalanced conditions is evaluated using MATLAB/Simulink and SimPowerSystem environment. For Three-phase, bidirectional rectifier, the system parameters are: Peak Input Phase Voltage = 155.6 V, 50Hz. Boost inductance = 1mH, Operating frequency is 5 KHz. The desired DC-link voltage of the proposed rectifier is set at 400 V.

IV a) Performance Evaluation for Unbalanced Mains

This technique is analyzed even under more unbalanced conditions as multiple case study. The controller is tested by introducing voltage magnitude unbalance of peak input phase voltage 40 V in phase C and peak input phase voltage 155.6 V

in phases, A and B. Comparative results from fig. 5 reveal that under unbalanced mains condition, there is low input power factor, high input current THD without controller. With proposed controller, the maximum THD of the source (line) current is reduced to just 4.86% from 8.56%, which is well within acceptable limits. Further with the proposed algorithm, there is no reduction in DC bus voltage and ripple content is negligible. This algorithm is also analyzed by introducing voltage magnitude unbalance of peak input phase voltage 70 V in phase B and peak input phase voltage 155.6 V in phases, A and C. Comparative results from fig. 6 reveal low input power factor, high input current THD without proposed algorithm. With proposed algorithm, the maximum THD of the source current is reduced to just 3.04% from 5.75% and at the same time has unity input power factor with well-regulated DC bus voltage and negligible ripple content. The controller is tested by introducing voltage magnitude unbalance of peak input phase voltage 50 V in phase C and peak input phase voltage 155.6 V in phases, A and B as shown in fig. 7. Results reveal that under such conditions in conventional converter, there is low input power factor, high input current THD. With proposed controller, the maximum THD of the source current is reduced to just 4.29% from 7.52%. Moreover with the proposed algorithm, there is no reduction in DC bus voltage and ripple content is negligible. At time $t=0.5$ second, the controller is tested for unbalanced sag in all phases by introducing voltage magnitude unbalance of peak input phase voltage 90 V in phase A, peak input phase voltage 110 V in phase B and peak input phase voltage 120 V in phase C. Simulations for unbalanced sag without controller and with controller are carried out. Results from fig. 8 reveal that under unbalanced mains condition, there is low input power factor, high input current THD without proposed controller. With proposed controller, the maximum THD of the source currents I_a, I_b, I_c is reduced to just 2.96% from 8.19% which is well within acceptable limits and makes the converter almost free of harmonics pollution. With the implementation of proposed technique, even under unbalance mains condition, IPQC works in same manner as that for balanced mains conditions having unity input power factor, low input current THD, with balanced currents drawn by rectifier and regulated DC output voltage and reduced ripple content of output voltage.

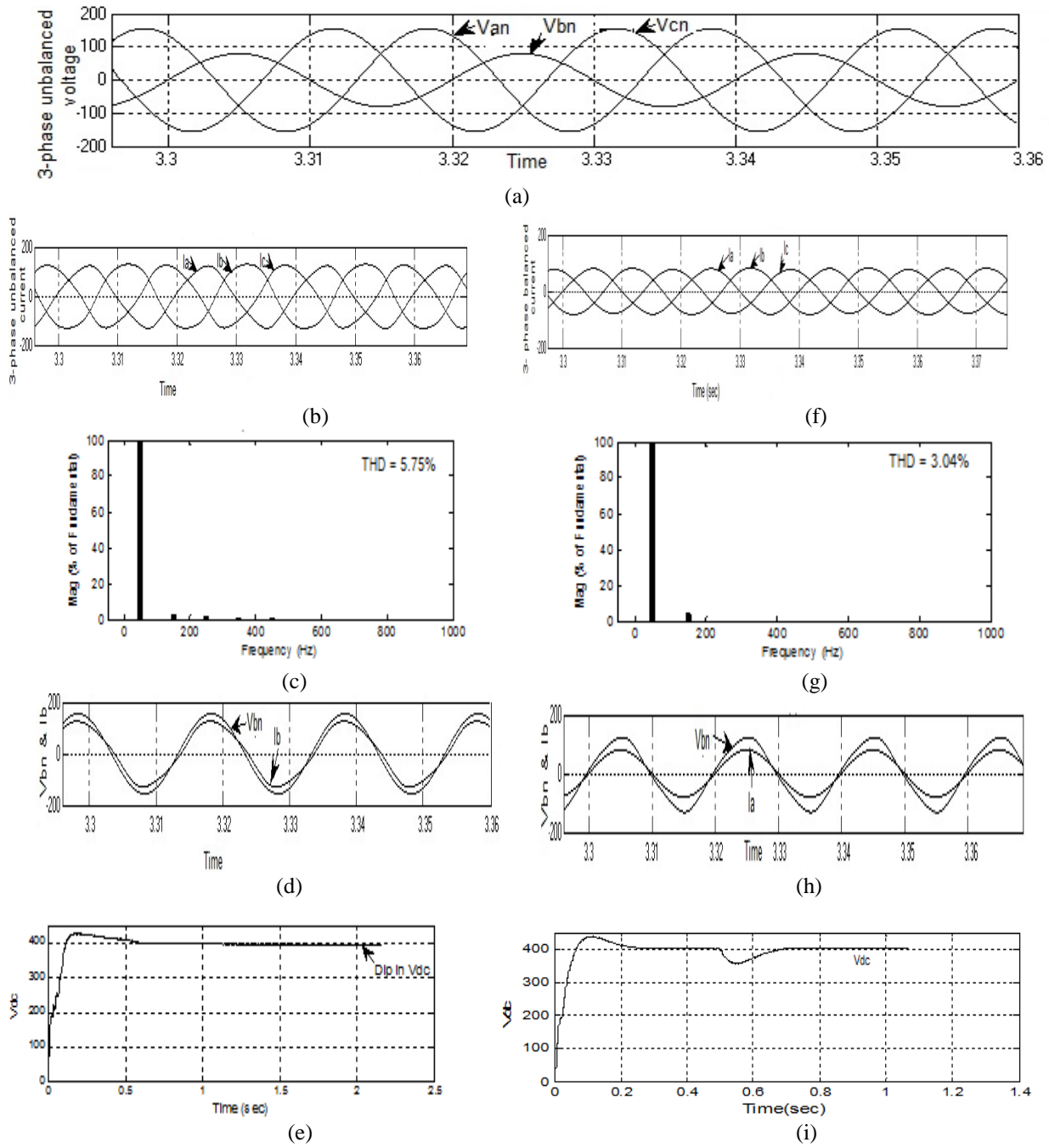
Fig. 5 Waveforms for IPQC with conventional controller and with proposed controller for sag in phase ‘A’



- 5(a) Three-phase voltages with sag in phase A without proposed algorithm
- (b) Three-phase unbalanced currents drawn by rectifier.
- (c) High THD of source currents Ia, Ib, Ic.
- (d) Source voltage & current for phase ‘A’ with low input power factor.
- (e) High ripple and dip in DC-bus voltage.

- (f) Three-phase balanced currents drawn by rectifier with proposed control algorithm
- (g) THD of source currents Ia, Ib, Ic.
- (h) Source voltage & current for phase ‘A’ with near unity supply power factor
- (i) Regulated and reduced-rippled DC bus voltage.

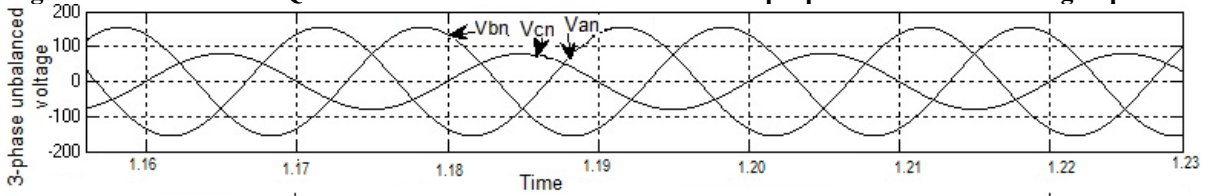
Fig. 6 Waveforms for IPQC with conventional controller and with proposed controller for sag in phase ‘B’



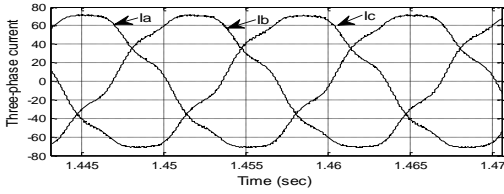
- 6(a) Three-phase voltages with sag in phase B without rectifier proposed algorithm
- (b) Three-phase unbalanced currents drawn by rectifier.
- (c) High THD of source currents Ia, Ib, Ic.
- (d) Source voltage & current for phase ‘A’ with low input power factor.
- (e) High ripple and dip in DC-bus voltage.

- (f) Three-phase balanced currents drawn by with proposed control algorithm
- (g) THD of source currents Ia, Ib, Ic.
- (h). Source voltage & current for phase ‘A’ with near unity supply power factor
- (i) Regulated and reduced-rippled DC bus voltage.

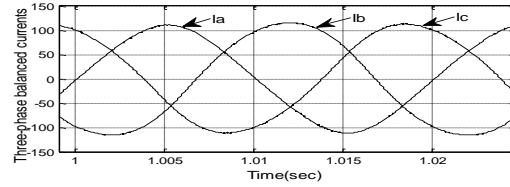
Fig. 7 Waveforms for IPQC with conventional controller and with proposed controller for sag in phase ‘C’



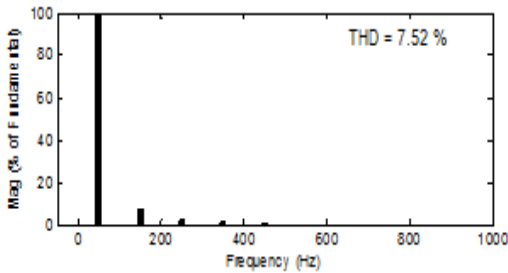
(a)



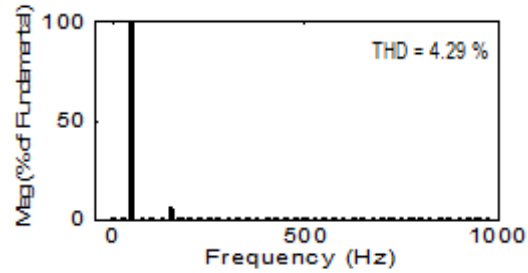
(b)



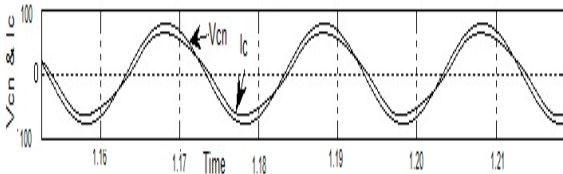
(f)



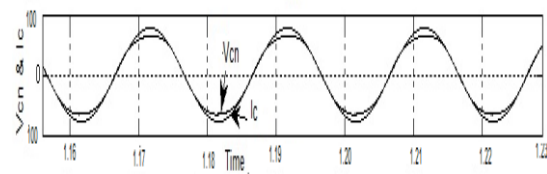
(c)



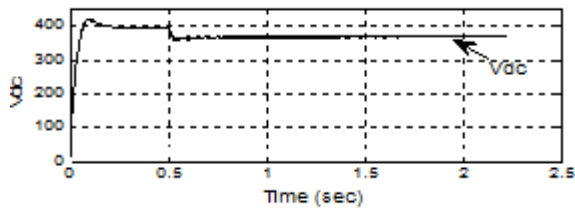
(g)



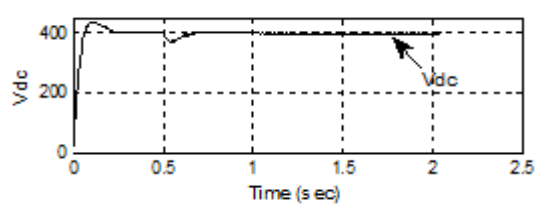
(d)



(h)



(e)

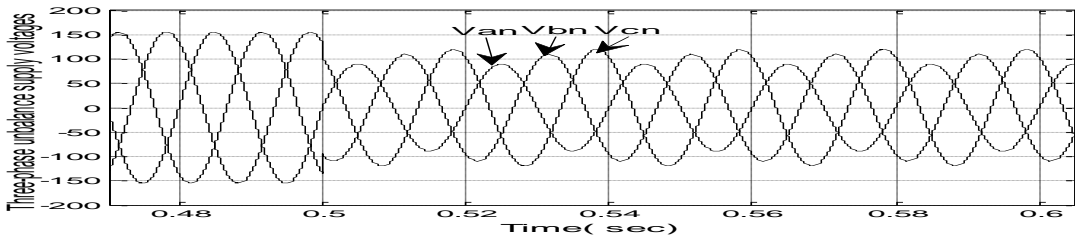


(i)

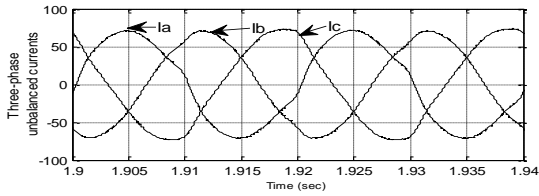
- 7(a) Three-phase voltages with sag in phase C without proposed algorithm
- (b) Three-phase unbalanced currents drawn by rectifier.
- (c) High THD of source currents Ia, Ib, Ic.
- (d) Source voltage & current for phase ‘A’ with low input power factor.
- (e) High ripple and dip in DC-bus voltage.

- (f) Three-phase balanced currents drawn by rectifier with proposed control algorithm
- (g) THD of source currents Ia, Ib, Ic.
- (h). Source voltage & current for phase ‘A’ with near unity supply power factor
- (i) Regulated and reduced-rippled DC bus voltage.

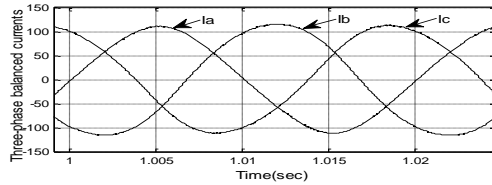
Fig. 8 Waveforms for IPQC with conventional controller and with proposed controller for unbalanced phase voltages.



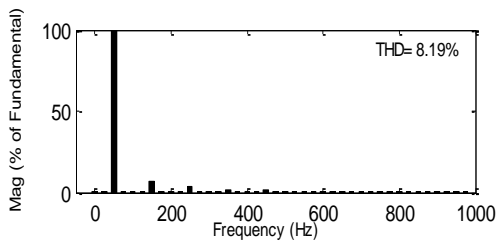
(a)



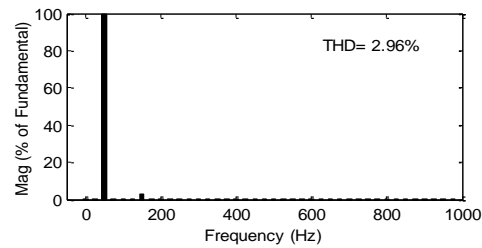
(b)



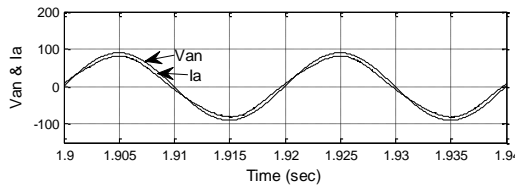
(f)



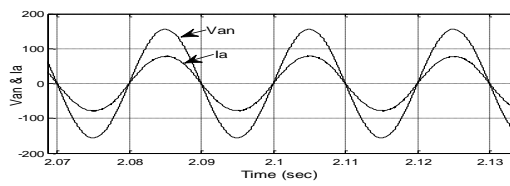
(c)



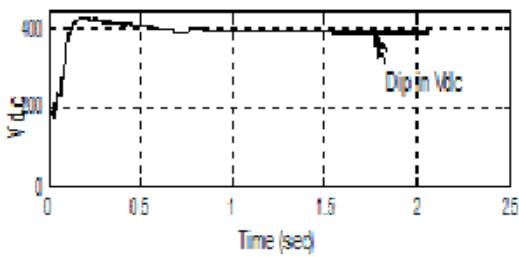
(g)



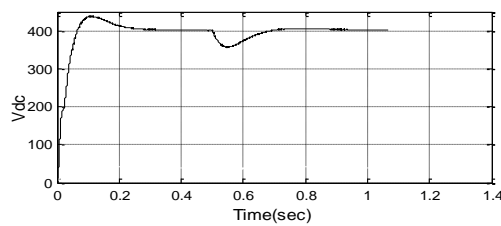
(d)



(h)



(e)



(i)

- 8(a) Three-phase voltages with unbalance introduced at $t=0.5\text{sec}$ without proposed algorithm
 (b) Three-phase unbalanced currents drawn by rectifier.
 (c) High THD of source currents I_a, I_b, I_c .
 (d) Source voltage & current for phase 'a', with low input supply power factor.
 (e) High ripple and dip in DC-bus voltage

- (f) Three-phase balanced currents drawn by rectifier with proposed algorithm
 (g) THD of source currents I_a, I_b, I_c .
 (h).Source voltage & current for phase 'a', with near unity supply power factor
 (i)Regulated and reduced-rippled DC bus voltage.

IVb) Performance Evaluation under Harmonics Distortion. The controller is tested by introducing harmonics up to 9th order, rest all parameters are same as rated. Fig. 9a) shows three-phase supply voltages with injected harmonics up to 9th order, Fig.9f) Shows source voltage & current for phase ‘A’ with proposed control algorithm which depicts nearly supply power factor, Fig.9g) depicts three-phase balanced currents

drawn by rectifier, Fig.9h) shows the harmonic spectrum of input current. The harmonic input current waveform shows %THD(Ia)=4.68%, %THD(Ib)=4.88%, %THD(Ic)=4.78%, which is well within acceptable limits. Fig.9i) shows regulated and reduced-rippled DC-bus voltage with proposed controller.

Fig.9 Waveforms for IPQC with conventional controller and with proposed controller for injected harmonics

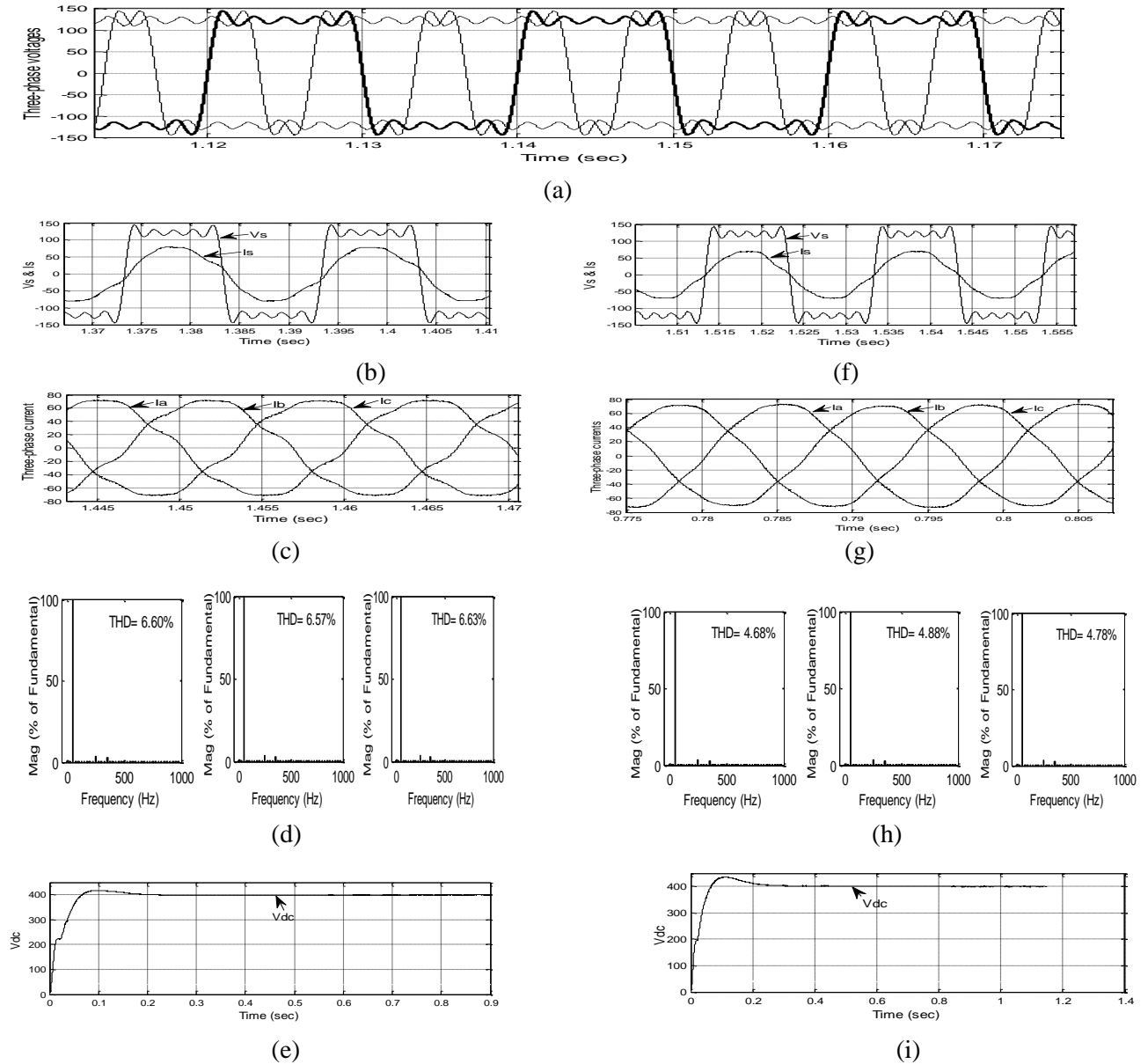


Fig:9(a) Injected harmonics upto 9th order in all phases without proposed controller
 (b) Three-phase unbalanced currents drawn by rectifier.
 (c) High THD of source currents Ia, Ib, Ic.
 (d) Source voltage & current for phase ‘a’, with low input supply power factor.
 (e) High ripple and dip in DC-bus voltage

(f) Three-phase balanced currents drawn by rectifier with proposed controller
 (g) THD of source currents Ia, Ib, Ic.
 (h) Source voltage & current for phase ‘a’, with near unity supply power factor
 (i) Regulated and reduced-rippled DC bus voltage

IV c) Performance Evaluation by introducing both Harmonics and Sag in AC Mains.

The controller is also tested by introducing harmonics upto 9th order in all phases and a sag of 90 volts(45% sag) in phase A only, rest all parameters are same as rated. Fig. 10a) shows a three-phase voltage with injected harmonics upto 9th order in all phases and with 45% sag in phase 'A' i.e. 90 volts. Fig. 10b) shows source voltage & current for phase 'A' after the implementation of proposed control algorithm which shows nearly unity input power factor. Fig. 10 c) shows the THD of source currents Ia, Ib, Ic without proposed

controller which is 9.10 %, 7.24 %, 7.24% respectively, Fig. 10e) depicts the THD of source currents Ia, Ib, Ic with proposed controller which is 4.81 %, 4.88 %, 4.85% respectively. It is well within acceptable limits and makes the converter almost free of harmonics pollution. Fig. 10 d) shows unregulated DC bus voltage with high ripple content without proposed algorithm. Fig. 10f) shows well-regulated and reduced-rippled DC bus voltage with proposed algorithm.

Fig.10 Waveforms for IPQC with conventional controller and with proposed controller for injected harmonics and sag

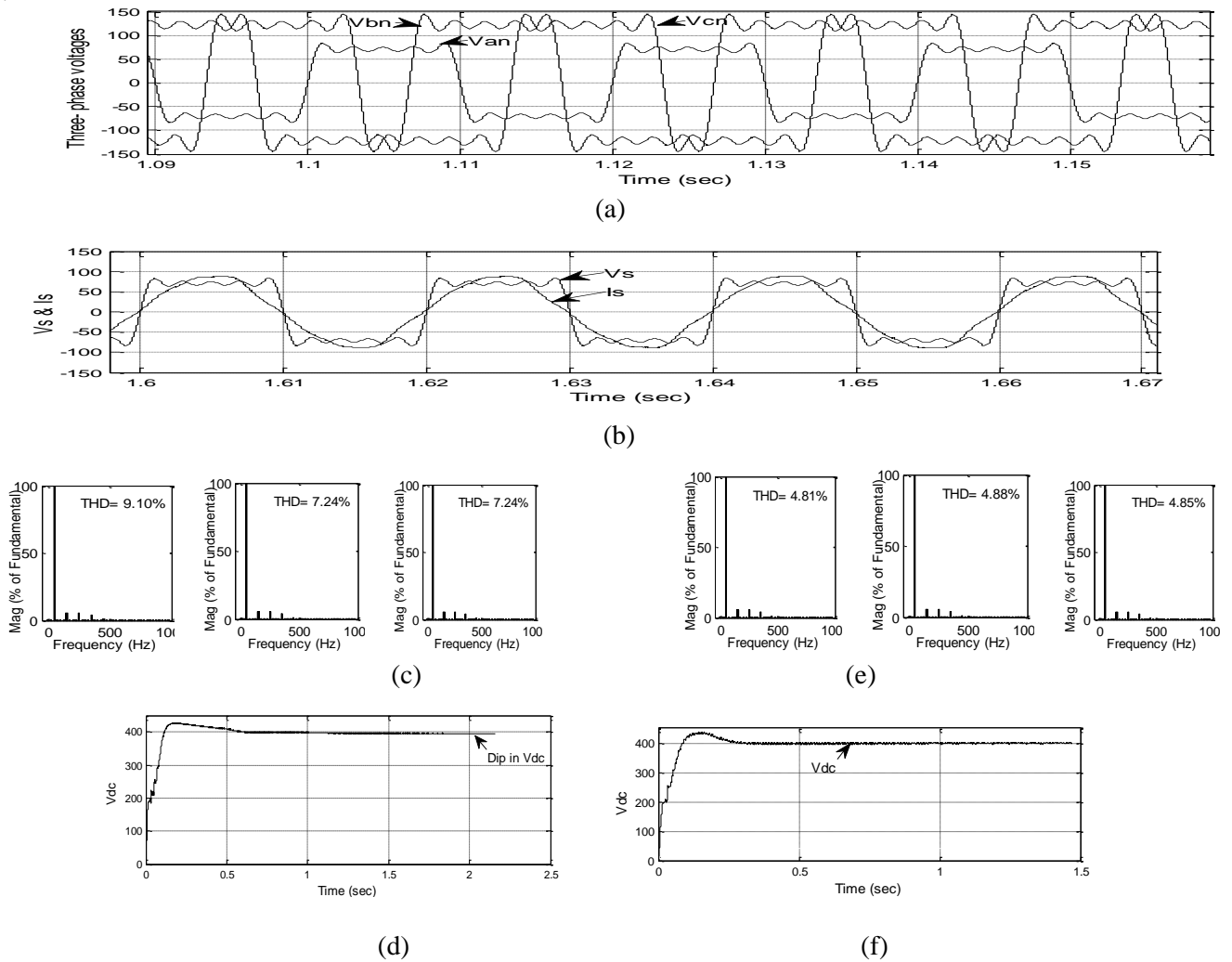


Fig: 10 a) Three-phase main voltages with harmonics injected and sag 45% in phase A.
 b) Source voltage & current for phase 'a', with near input supply power factor with proposed controller
 c) THD of source currents Ia, Ib, Ic without proposed controller.
 d) High ripple and dip in DC-bus voltage.
 e) THD of source currents Ia, Ib, Ic with proposed controller.
 f) Regulated and reduced-rippled DC bus voltage

IV d) Performance Evolution under Phase Angle Deviations

With the proposed algorithm, the controller is tested by introducing phase difference between phases, rest all parameters are same as rated. Phase B is taken at -90° and phase C is taken at $+90^\circ$. Fig. 11(a) shows three-phase supply voltages displaced in phase angles. Fig.11(b) shows three-phase line currents without proposed controller. Fig. 11(c) shows the harmonic spectrum of input currents without proposed controller which is for $I_a=6.58\%$, $I_b=5.93\%$, $I_c=7.2\%$. Fig.11(d)

shows three-phase line currents with proposed controller. Fig.(e) shows the harmonic spectrum of input currents with proposed controller which is for $I_a=4.75\%$, $I_b=4.87\%$, $I_c=4.89\%$ respectively which are well within acceptable limits. Fig.11(f) shows high ripple and dip in DC bus voltage without proposed controller and Fig.11 (g) shows well-regulated and reduced-rippled DC bus voltage with proposed controller.

Fig.11 Waveforms for IPQC with conventional controller and with proposed controller for Phase Angle Deviations

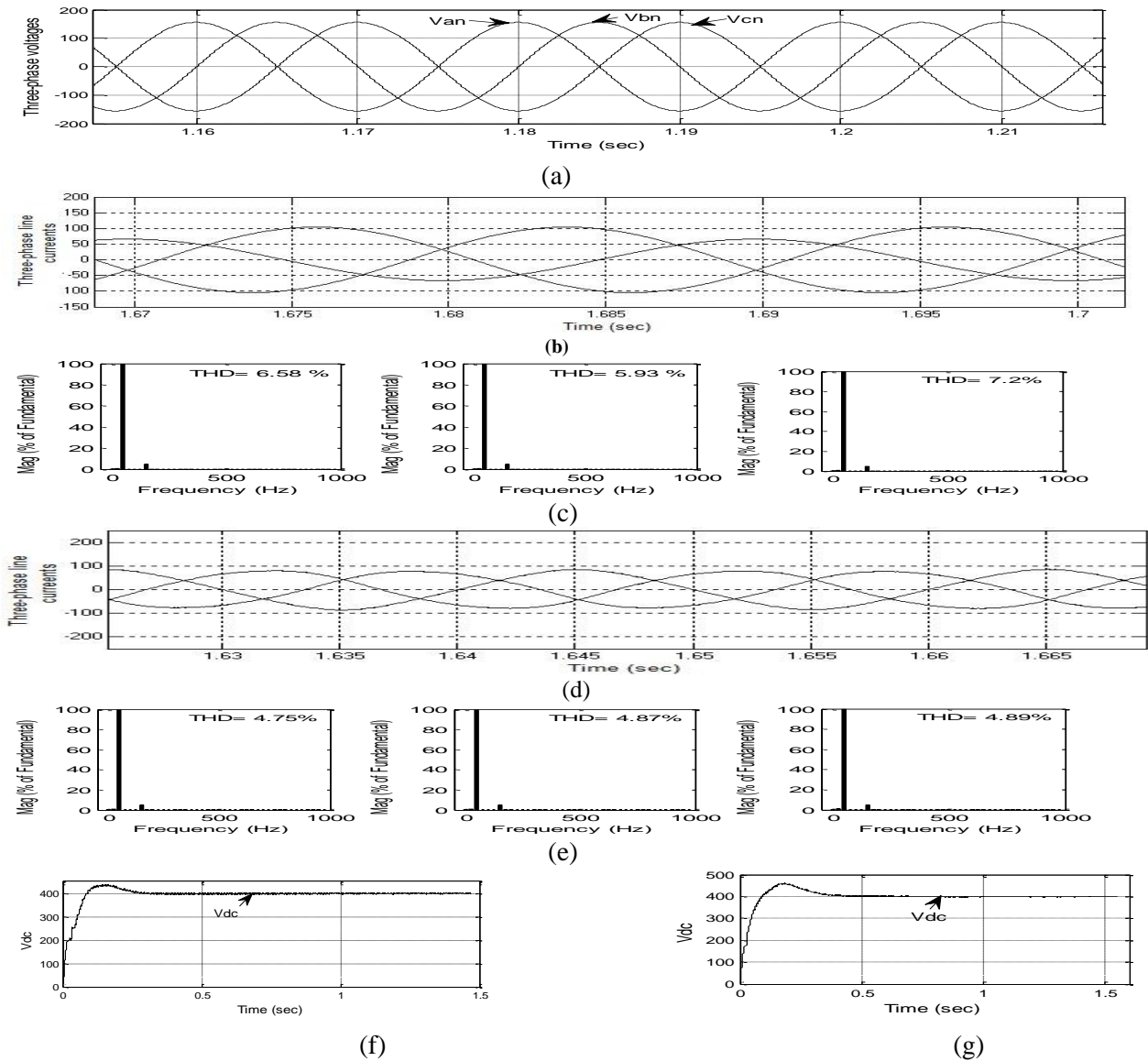


Fig.11 a) Source Voltage displaced in phases ('b' & 'c') by 90°
 b) Three-phase line currents without proposed controller
 c) THD of source currents I_a, I_b, I_c without proposed controller. f) High ripple and dip in DC-bus voltage
 d) Three-phase line currents with proposed controller
 e) THD of source currents I_a, I_b, I_c with proposed controller.
 g) Regulated and reduced-rippled DC bus voltage

IVe) Performance Evaluation under Load Perturbation

The controller is tested by introducing load perturbation from 40 A to 66.66 A (step increase in load) at $t=0.7$ sec. and from 40 A to 25 A (step decrease in load) at $t=1.2$ sec. with rated source voltage and current. Fig.12 a) shows load voltage and load current

waveforms for step increase and step decrease in load without proposed controller. The waveforms shows high ripple and dip in DC-bus voltage. Fig.12 b) shows load voltage and load current waveforms for step increase and step decrease in load with proposed

controller. It shows less ripple with regulated DC-bus voltage. There is very small undershoot and overshoot in load voltage and load current settles at reference value very quickly. Fig.12 c) shows source voltage and current for phase 'A' with proposed controller. After the implementation of proposed control algorithm which shows nearly unity input power factor.

Fig.12d) shows the harmonic spectrum of input currents with proposed controller, this harmonic spectrum depicts THD of source currents I_a , I_b , I_c as 0.89%, 0.88%, 0.98% respectively which are well within acceptable limits and makes the converter almost free of harmonics pollution.

Fig.12 Waveforms for IPQC with conventional controller and with proposed controller for Load Perturbation

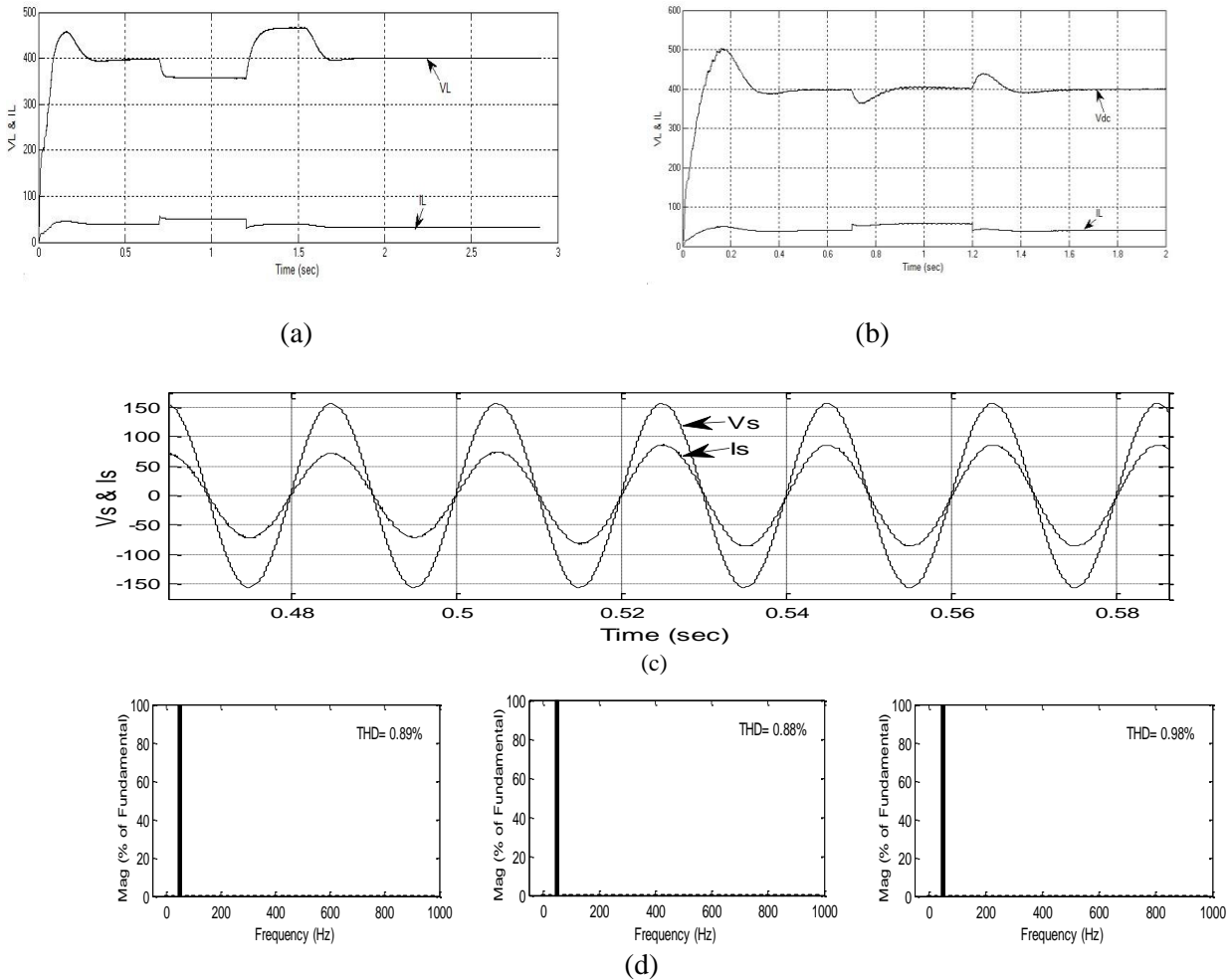


Fig. 12a) Waveform for load perturbation for step increase in load and step decrease in load without proposed controller
 b) Waveform for load perturbation for step increase in load and step decrease in load with proposed controller
 c) Source Voltage and line current for phase 'A' with proposed controller .
 d) THD of source currents I_a , I_b , I_c with proposed controller.

V. CONCLUSION

The proposed scheme based on Clarke retransformation provides compensation for supply and load perturbations, which are practically encountered in real power systems. Instead of insensitivity to it which has been the basis of most of the control schemes reported in the literature, the improved performance of rectifier is well established by the simulation results under

different load as well as supply conditions. Simulation results are explored using Matlab/Simulink software. Relevant figures and graphs have been shown to understand the conclusive results for the simulation model. The source current harmonics are compensated very effectively by using the proposed technique and also at the same time maintaining unity input power

factor, low input current THD and regulated DC output voltage. The proposed control algorithm proves to be

very effective in addressing the supply and load perturbations faced in real time.

VI. REFERENCES

- [1] Dixon J. W., "Boost type PWM rectifiers for high power applications," Ph.D dissertation, Dept. Elect. Comput. Eng., McGill Univ., Montreal, QC, Canada, Jun. 1988.
- [2] Fuld B., Kern S., and Ridley R., "A combined buck and boost power-factor-controller for three-phase input," in Power Electronics and Applications, European Conference, Sep. 1993.
- [3] Draft-Revision of Publication IEC 555-2: Harmonics, Equipment for Connection to the Public Low Voltage Supply System. IEC SC 77A, 1990.
- [4] IEEE Recommended Practices and Requirements for Harmonics Control in Electric Power Systems, IEEE std. 519, 1992.
- [5] N. Balbo and L. Malesani "Hybrid Active Filter for Parallel Harmonic Compensation", *EPE 1993*, pp.133 -138 1993.
- [6] Lai J. S. and Peng F. Z., "Multilevel converters: A New Breed of Power Converters", *IEEE Trans. on Industry Application*, vol. IA-32, No. 3, May/June 1996, pp. 509-517
- [7] B. Singh, K. Al. Hadda, and A. Chandra, "A review of active filter for power quality improvement," *IEEE Trans. Ind. Electron.*, vol 46, pp.960-971, Oct. 1999.
- [8] Fujita H., Yamasaki T., and Akagi H., "A hybrid active filter for damping of resonance in industrial power system", *IEEE Trans. On Power Electronics*, vol 15, no. 2, Mar. 2000, pp. 215- 222.
- [9] Chen C., and Hsu Y., "A novel approach to the design of a shunt active filter for an unbalanced three-phase four-wire system under non-sinusoidal conditions", *IEEE Trans., On Power Delivery*, vol. 15, no.4, Oct. 2000, pp. 1258-1264.
- [10] M. McGranaghan, D. Mueller, and M. Samotyj, "Voltage sags in industrial systems," *IEETrans.Ind. Appl.*, vol. 29, no. 2, pp. 397-403, Mar./Apr. 1993.
- [11] M. Basseville and I. Nikiforov, Detection of Abrupt Changes.—*Theory and Application*. Englewood Cliffs, NJ: Prentice-Hall, Apr. 1993.
- [12] J.-K. Kang, S.-K. Sul, and S.-D. Kwanak-Ku, "Control of unbalanced voltage PWM converter using instantaneous ripple power feedback," in *IEEE Conference*, 1997, pp. 503-508.
- [13] L. Zhang, "Three-phase unbalance of voltage dips," Licentiate thesis, Dept. Elect. Power Eng., Chalmers Univ. Technol., Gothenburg, Sweden, Nov. 1999.
- [14] H.-S. Song and K. Nam, "Dual current control scheme for PWM converter under unbalanced Input voltage conditions," *IEEE Trans. Industrial Electronics*, vol. 46, no. 5, pp. 953-959, Oct. 1999.
- [15] M. Bollen and L. Zhang, "A method for characterization of three phase unbalanced dips from recorded voltage waveshapes," in Proc. *IEEE Telecommunication Energy Conf.*, Jun. 1999, p. 93.
- [16] M. H. J. Bollen and S. Styvaktakis, "Characterization of three-phase unbalanced sags, as easy as one, two, three," presented at the *IEEE Power Eng. Soc. Summer Meeting*, Seattle, WA, Jul. 2000.
- [17] Assessment of Voltage Unbalance, Annette von Jouanne, Senior Member, IEEE and Basudeb (Ben) Banerjee, Member, *IEEE transactions on power delivery*, vol. 16, no. 4, october 2001.
- [18] E. Styvaktakis, "Automating power quality analysis," Ph.D. dissertation, Chalmers Univ. of Technol., Gothenburg, Sweden, 2002.
- [19] T. Andersson and D. Nilsson, "Test and evaluation of voltage dip immunity" Sweden, 2002, STRI Rep..
- [20] M. H. J. Bollen and L. D. Zhang, "Different methods for classification of three-phase unbalanced voltage dips due to faults," *Elect. Power Syst. Res.*, vol. 66, no. 1, pp. 59-69, Jul. 2003.
- [21] P. Heine and M. Lehtonen, "Voltage sag distributions caused by power system faults," *IEEE Trans. Power Del.*, vol. 18, no. 4, pp. 1367-1373, Nov. 2003.
- [22] R. Leborgne, G. Olguin, and M. Bollen, "The influence of pq-monitor connection on voltage dip measurement," in *Inst. Elect. Eng.—MedPower*, Cyprus, Nov. 2004.
- [23] M. Bollen, Understanding Power Quality Problems: Voltage Sags and Interruptions. *New York: Wiley-IEEE Press*, 1999.
- [24] T. Rakesh I, V. Madhusudhan, M. Sushama, MI Control of MLI-DSTATCOM for Sag and Swell Enhancement in Power Distribution System. *International Electrical Engineering Journal (IEEJ)* Vol. 7 (2016) No.6, pp. 2279-2285
- [25] N. Bachschmid, P. Pennacchi, and A. Vania, "Diagnostic significance of orbit shape analysis and its application to improve machine fault detection," *J. Braz. Soc. Mech. Sci. & Eng.*, vol. 26, no. 2, Apr./Jun. 2004, Rio de Janeiro, Brazil.
- [26] V. Ignatova, P. Granjon, S. Bacha, and F. Dumas, "Classification and characterization of three phase voltage dips by space vector methodology," presented at the *FPS Conf.*, 2005.
- [27] A. H. Bhat and P. Agarwal, "Three-phase, power quality improvement AC-DC converters," *Elsevier Electric Power Systems Research*, pp. 276-289, 2008.
- [28] Nitin Langer, Abdul Hamid Bhat Supply Perturbation Compensated Control Scheme for Three- Phase IPQC rectifier *International journal of Electrical Power and Energy Systems* Vol:54, pp:17- 25, 2014.
- [29] S.N. Ghani, "Digital Computer Simulation of Three- Phase Induction Machine Dynamics A Generalized Approach", *IEEE Trans Industry Appl.*, Vol. 24, No. 1, pp. 106-114, 1988.
- [30] Parag Kanjiya, Bhim Singh, Ambrish Chandra, Kamal Al-Haddad, Fellow IEEE, "SRF theory revisited to control self-supported dynamic voltage restorer (DVR) for unbalanced and nonlinear loads" *IEEE Transactions on Industry Applications*, Vol.49, No. 5, September/October 2013.
- [31] Sathish Babu P, Kamaraj N, "Performance Investigation of Dynamic voltage restorer using PI and fuzzy logic controller" in international conference on Power, Energy and Control (ICPEC), IEEE 2013.
- [32] Ebrahim Babaei, Mohammad Farhadi, Kangarlu, Mehran Sabahi "Mitigation of Voltage Disturbances Using Dynamic Voltage Restorer Based on Direct Converters" in *IEEE Transactions on Power Delivery*, Volume: 25, Issue: 4, Oct. 2010.
- [33] Kelly Caroline Mingorancia de Carvalho, Naji Rajai Nasri Ama, Wilson Komatsu, Fernando Ortiz Martinz, Ricardo Souza Figueredo, Sao Paulo, "Disturbance calculation based on space vector dot product: Applications to compensators" *Power Electronics Conference (IPEC-Hiroshima 2014 - ECCE-ASIA)*, 2014 International
- [34] k.berrahal a. bouhental a.bensalem "reactive power compensation with five level based inverter *Journal of Electrical Engineering* : volume 16 / 2016 - edition : 4 pages 340-347
- [35] Saribulut, L. ; Tumay, M. "A robust SVM technique to minimize the effects of unbalanced voltage disturbances " *Electrical and Electronics Engineering*, 2009. *ELECO 2009. International Conference on Publication Year: 2009* , Page(s): I-283 - I-287.